PHYSICAL REVIEW D VOLUME 22, NUMBER 7 1 OCTOBER 1980

Three-neutrino oscillations and present experimental data

V. Barger and K. Whisnant
Physics Department, University of Wisconsin, Madison, Wisconsin 53706

R. J. N. Phillips
Rutherford Laboratory, Chilton, Didcot, Oxon, England
(Received 2 June 1980)

Indications of neutrino oscillation effects in reactor, beam-dump, deep-mine, and solar-neutrino experiments are discussed. Assuming three neutrinos, oscillation probabilities and/or limits are extracted from the data. We present classes of solutions that can explain the observed effects.

I. INTRODUCTION

Neutrino oscillations[1,2] are of great interest because of the light they may shed on neutrino mass scales and mixing angles. A fresh round of more accurate measurements is currently running or being planned, but there are already indications of oscillation effects in reactor, beam-dump, deep-mine, and solar-neutrino experiments. In the present paper we discuss classes of solutions previously proposed[3] to explain some or all of these effects and explore their consequences for other experiments, assuming three neutrinos.[4,5]

II. FORMALISM

In general, the neutrino mass eigenstates ν_i with masses m_i differ from the weak-charged-current eigenstates ν_α (distinguished here by Greek suffixes). The two sets of states are related by a unitary transformation $|\nu_\alpha\rangle = \mathfrak{U}_{\alpha i}|\nu_i\rangle$. Hence, if we initially have ν_α with momentum p, the transition amplitude A and probability P for observing ν_β after time t are

$$\begin{aligned} A(\nu_\alpha \to \nu_\beta) &= \sum_{i=1}^{n} \mathfrak{U}_{\alpha i}\mathfrak{U}^*_{\beta i}\exp(-iE_i t)\,, \\ P(\nu_\alpha \to \nu_\beta) &= |A(\nu_\alpha \to \nu_\beta)|^2\,, \end{aligned} \tag{1}$$

where n is the number of eigenstates and $E_i^2 = p^2 + m_i^2$. For the cases of interest where $p \gg m_i$, the amplitude for a flight path length L can be written

$$A(\nu_\alpha \to \nu_\beta) = \delta_{\alpha\beta} + \sum_{i\neq j} \mathfrak{U}_{\alpha i}\mathfrak{U}^*_{\beta i}[\exp(-i\Delta_{ij}) - 1]\,, \tag{2}$$

where $\Delta_{ij} = \frac{1}{2}(m_i^2 - m_j^2)L/E$ and one particular state j has been singled out arbitrarily. Interference between different terms in A gives oscillatory contributions to P. Note that if a matrix element $\mathfrak{U}_{\alpha i}$ is very small, ν_α oscillations have essentially no Δ_{ij} components.

For antineutrinos replace $\mathfrak{U}$ by $\mathfrak{U}^*$. Hence

$$P(\nu_\alpha \to \nu_\beta) = P(\bar\nu_\beta \to \bar\nu_\alpha)\,, \tag{3}$$

where this relation may be seen as CPT invariance. In general, $\nu_\alpha \to \nu_\beta$ transitions are not required to be the same as $\nu_\beta \to \nu_\alpha$ and $\bar\nu_\alpha \to \bar\nu_\beta$ for $\alpha \neq \beta$, but equality holds here too for $n = 2$ neutrinos or when $\mathfrak{U}$ is real (CP conservation), and in some other simple situations such as the leading oscillations and averaged oscillations discussed below.

If the mass eigenstates are Dirac particles, ν_i and ν_α are four-component spinors. If, instead, the mass eigenstates are Majorana particles $\nu_i = \bar\nu_i$, the weak eigenstates are to be interpreted as left- and right-handed projections

$$\begin{aligned} \nu_{\alpha L} &= \sum_{i=1}^{n} \tfrac{1}{2}(1+\gamma_5)\mathfrak{U}_{\alpha i}\nu_i\,, \\ \bar\nu_{\alpha R} &= \sum_{i=1}^{n} \tfrac{1}{2}(1-\gamma_5)\mathfrak{U}^*_{\alpha i}\nu_i\,. \end{aligned} \tag{4}$$

Provided the weak current contains no right-handed neutrino couplings, as we shall assume here, no appreciable neutrino-antineutrino mixing occurs.[6] When both Majorana and Dirac mass terms are present in the Lagrangian,[7] the possibility exists for oscillations which mix neutrino members of weak doublets and singlets,[8] as well as oscillations which mix flavors. Our principal interest in this paper is in flavor-changing oscillations, though we will briefly consider doublet-singlet mixing at a later point.

The oscillations are periodic in L/E. With L/E in m/MeV and m_i in eV units, the oscillation argument in radians is

$$\tfrac{1}{2}\Delta_{ij} = 1.27\,\delta m^2_{ij}\,L/E\,, \tag{5}$$

where $\delta m^2_{ij} \equiv m_i^2 - m_j^2$. Oscillations arising from a given δm^2_{ij} can be most readily mapped out at L/E values of order $1/\delta m^2_{ij}$. The presently accessible ranges of L/E in m/MeV are ~10^{10} (solar), ~$10-10^5$ (deep mine), 1–7 (low-energy accelerators), 1–20 (reactors), 0.3–3 (meson factories), and 0.01–0.05 (high-energy accelerators).

The leading oscillation—the first to occur as L/E increases from zero—is controlled by the largest mass differences only, and has a particularly simple form if one mass-squared difference dominates. Suppose that the largest eigenmass value m_n is separated from the others, such that $|\delta m^2{}_{in}| \gg |\delta m^2{}_{ij}|$ for $i, j \neq n$. Then the leading oscillation is given simply by the terms involving $\delta m^2{}_{in}$ with all other mass differences set essentially to zero:

$$A(\nu_\alpha \to \nu_\beta) = \delta_{\alpha\beta} + (\delta_{\alpha\beta} - \mathcal{U}_{\alpha n}\mathcal{U}^*_{\beta n})(e^{-i\Delta} - 1)\,, \qquad (6)$$

$$P(\nu_\alpha \to \nu_\alpha) = 1 - 4(|\mathcal{U}_{\alpha n}|^2 - |\mathcal{U}_{\alpha n}|^4)\sin^2(\tfrac{1}{2}\Delta)\,, \qquad (7)$$

$$\begin{aligned} P(\nu_\alpha \to \nu_\beta) &= P(\nu_\beta \to \nu_\alpha) \\ &= 4|\mathcal{U}_{\alpha n}|^2 |\mathcal{U}_{\beta n}|^2 \sin^2(\tfrac{1}{2}\Delta) \quad \text{for } \alpha \neq \beta\,, \end{aligned} \qquad (8)$$

where $\Delta = \frac{1}{2}\delta m_{in}{}^2 L/E$. Hence the n^2 different neutrino transition probabilities are governed by a single oscillatory factor $\sin^2(\frac{1}{2}\Delta)$ and the coefficient factors $|\mathcal{U}_{\alpha n}|^2$ of which $n-1$ are independent. In this regime neutrino and antineutrino predictions are identical; no CP-violating phases in $\mathcal{U}_{\alpha i}$ can be detected. Notice that if $\mathcal{U}_{\alpha n} = 0$, neutrinos of type α take no part in the leading oscillations.

Asymptotic behavior is also rather simple. At sufficiently large values of L/E, where all Δ_{ij} arguments have been through many cycles, detectors cannot resolve individual oscillations and become sensitive only to average values, which are given by

$$\langle P(\nu_\alpha \to \nu_\beta)\rangle = \langle P(\bar\nu_\alpha \to \bar\nu_\beta)\rangle = \sum_i |\mathcal{U}_{\alpha i}\mathcal{U}^*_{\beta i}|^2\,. \qquad (9)$$

For n independent neutrinos, the minimal acheivable value for a diagonal term is

$$\langle P(\nu_\alpha \to \nu_\alpha)\rangle_{\min} = 1/n\,. \qquad (10)$$

The discussion above refers to oscillations in vacuum. Additional effects occur in matter[9] due to coherent forward ν_e-e charged-current scattering (neutral currents give no lowest-order effect in the standard Glashow-Salam-Weinberg theory). Matter effects have a characteristic wavelength L_M, independent of E,

$$L_M = (\rho_e G/2\pi)^{-1}\,, \qquad (11)$$

where ρ_e is the electron density. For typical rock, $\rho_e \simeq 12\times 10^{23}$ cm^{-3} and $L_M \simeq 1.2\times 10^7$ m. Matter corrections to vacuum oscillations become significant only when the matter oscillation length L_M is comparable or shorter than the vacuum oscillation length L_V for the smallest eigenmass-squared difference

$$L_M \lesssim L_V = \frac{4\pi E}{(\delta m^2)_{\min}}\,. \qquad (12)$$

For the corrections to be observable, the distance traversed in matter must also be an appreciable fraction of L_M. Hence, matter corrections are very small in all terrestrial contexts, except when neutrinos traverse a substantial fraction of the earth's diameter and have energies

$$E(\text{MeV}) \gtrsim 10^5[\delta m^2(\text{eV}^2)]_{\min}\,. \qquad (13)$$

III. THREE-NEUTRINO PARAMETRIZATION

We concentrate attention on the case $n=3$, since only three weak eigenstates ν_e, ν_μ, ν_τ are known. In this case the mixing matrix U can be parametrized by three angles θ_i with ranges $(0, \pi/2)$ and one CP-violating phase δ with range $(-\pi, \pi)$, following Ref. 10:

$$\begin{pmatrix} \nu_e \\ \nu_\mu \\ \nu_\tau \end{pmatrix} = \begin{pmatrix} c_1 & s_1c_3 & s_1s_3 \\ -s_1c_2 & c_1c_2c_3 + s_2s_3e^{i\delta} & c_1c_2s_3 - s_2c_3e^{i\delta} \\ -s_1s_2 & c_1s_2c_3 - c_2s_3e^{i\delta} & c_1s_2s_3 + c_2c_3e^{i\delta} \end{pmatrix} \begin{pmatrix} \nu_1 \\ \nu_2 \\ \nu_3 \end{pmatrix}, \qquad (14)$$

where $c_i = \cos\theta_i$, $s_i = \sin\theta_i$. The explicit formulas for $P(\nu_\alpha \to \nu_\beta)$ in terms of these parameters are lengthy and not particularly enlightening.

The leading oscillation formulas involve one oscillatory term $\sin^2(\frac{1}{2}\Delta)$ and two independent coefficients, which can be parametrized by two angles α and β. Denoting $P(\nu_\alpha \to \nu_\beta)$ by $P(\alpha \to \beta)$, we have

$$\begin{aligned} P(e \to e) &= 1 - \sin^2 2\alpha \sin^2\tfrac{1}{2}\Delta\,, \\ P(\mu \to \mu) &= 1 - 4\sin^2\alpha \cos^2\beta(1 - \sin^2\alpha\cos^2\beta)\sin^2\tfrac{1}{2}\Delta\,, \\ P(\tau \to \tau) &= 1 - 4\sin^2\alpha \sin^2\beta(1 - \sin^2\alpha\sin^2\beta)\sin^2\tfrac{1}{2}\Delta\,, \\ P(e \to \mu) &= \sin^2 2\alpha \cos^2\beta \sin^2\tfrac{1}{2}\Delta\,, \\ P(e \to \tau) &= \sin^2 2\alpha \sin^2\beta \sin^2\tfrac{1}{2}\Delta\,, \\ P(\mu \to \tau) &= \sin^2 2\beta \sin^4\alpha \sin^2\tfrac{1}{2}\Delta\,, \end{aligned} \qquad (15)$$

where $\frac{1}{2}\Delta = \frac{1}{4}\delta m_{31}{}^2 L/E \simeq \frac{1}{4}\delta m_{32}{}^2 L/E$ and m_3 is supposed to be the largest eigenmass. We have essentially parametrized the three linearly dependent coefficients $|U_{e3}|^2$, $|U_{\mu 3}|^2$, $|U_{\tau 3}|^2$ by $\cos^2\alpha$, $\sin^2\alpha\cos^2\beta$, $\sin^2\alpha\sin^2\beta$. Thus $\sin 2\alpha$ directly controls the amplitude of the $\nu_e \to \nu_e$ oscillation; $\cos\beta$ measures the relative amplitude of the $\nu_e \to \nu_\mu$ oscillation. When two oscillations are prescribed, all other leading oscillations are determined.

Asymptotic oscillation formulas are straightforward from Eqs. (9) and (14) and will not be written in generality. However, parameter values that minimize $\langle P(e\to e)\rangle$ are particularly interesting in view of the apparent severe deficiency of solar-neutrino events[11,12]: see Sec. IV below. The minimizing values are $c_1{}^2 = \frac{1}{3}$, $c_3{}^2 = \frac{1}{2}$ with θ_2 and δ free. The corresponding averaged values are

$$\begin{aligned}
&\langle P(e\to e)\rangle = \langle P(e\to\mu)\rangle = \langle P(e\to\tau)\rangle = \tfrac{1}{3}\,,\\
&\langle P(\mu\to\mu)\rangle = \langle P(\tau\to\tau)\rangle = \tfrac{1}{2} - \tfrac{2}{3}c_2{}^2 s_2{}^2\sin^2\delta\,, \qquad (16)\\
&\langle P(\mu\to\tau)\rangle = \tfrac{1}{6} + \tfrac{2}{3}c_2{}^2 s_2{}^2\sin^2\delta\,.
\end{aligned}$$

A fully symmetrical solution with all averaged values equal to $\frac{1}{3}$ is thus achieved with $c_2{}^2 = \frac{1}{2}$ and $\sin^2\delta = 1$ (maximal CP violation).[13-15]

If we impose a less stringent condition $\langle P(e\to e)\rangle < \frac{1}{2}$, the mixing parameters are constrained to a region approximated by the triangle $\theta_1 > 35°$, $\theta_1 - 45° < \theta_3 < 135° - \theta_1$, with θ_2 and δ free: See Fig. 1, which shows contours of $\langle P(e\to e)\rangle$ versus angles θ_1, θ_3. In much of our quantitative discussion of data we shall use solutions in this region. We shall also assume approximate CP conservation ($\sin\delta = 0$); however, Eqs. (14) and (16) show that

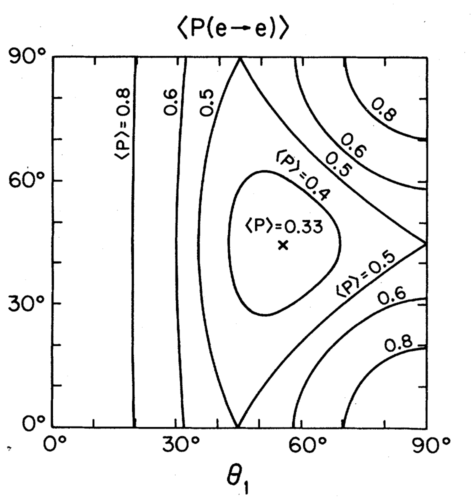

FIG. 1. Contour plot of $P(e\to e)$ vs weak-current angles θ_1 and θ_3.

suppressing this degree of freedom implies some loss of generality in the μ, τ sector.

IV. EXPERIMENTAL DATA

A. Solar neutrinos

The background ν_e flux around 1 MeV, measured in a well-shielded environment such as a mine, is dominated by fusion processes in the sun. Measurements[11] using the reaction $\nu_e + {}^{37}\mathrm{Cl} \to e^- + {}^{37}\mathrm{Ar}$ yielded a counting rate of 2.2 ± 0.4 solar-neutrino units (SNU) compared to a standard-solar-model prediction[12] of 7 SNU, where 1 SNU = 1 capture/sec per 10^{36} nuclei. This discrepancy suggests a neutrino-oscillation effect with

$$\langle P(e\to e)\rangle \sim 0.2\text{–}0.4 \quad \text{at } L/E \sim 10^{10}\ \mathrm{m/MeV}\,. \qquad (17)$$

We adopt this interpretation here.

To achieve such a near-minimal mean value with three neutrino flavors, the mixing angles θ_1 and θ_3 must lie near the minimizing solution of Sec. III and all mass differences must satisfy $\delta m^2 > 10^{-10}$ eV^2.

There is another conceivable scenario where $P(e\to e)$ itself oscillates downward with a wavelength of the order of the earth's orbital radius, controlled by a mass difference $\delta m^2 \sim 10^{-10}$ eV^2; in principle, the minimal value for a specific L/E is then zero.[16] However, the ^{37}Cl experiment integrates over a neutrino spectrum from 1 to 16 MeV, so an L/E average is more appropriate here anyway.

B. Deep-mine experiments

These experiments have measured high-energy muon production near the horizontal direction where the incident neutrinos come mostly from $\pi, K \to \mu \to e$ cascade decays near the earth's surface. About 120 events have been reported[17,18] within 40° of the horizontal direction, typically with $E \sim 10^4$ MeV, $L \sim 10^4\text{–}10^7$ m. In the Kolar gold field[17] the number of observed events is appreciably less than expected from standard weak-interaction theory. In the Johannesburg experiment,[18] the ratio of observed to expected ν_μ events was $0.62^{+0.17}_{-0.10}$. Although this evidence is not yet compelling, the results suggest that muon neutrinos may participate in substantial oscillations with $\delta m^2 \gtrsim 0.05$ eV^2. Upward events with $L \sim 10^7$ m can also be studied in deep-mine experiments.

C. Accelerator data

Searches have been made for $\nu_\mu \to \nu_e$ and $\nu_e \to \nu_e$ oscillations in high-energy neutrino beams. No positive effects have been seen. The Gargamelle experiment at the CERN proton synchrotron obtained[20]

$$P(\bar{\mu}\to\bar{e})/P(\mu\to\mu)<1.4\times10^{-3}\quad(90\%\,\mathrm{CL}), \tag{18}$$

$$P(\mu\to e)/P(\mu\to\mu)<1.3\times10^{-3}\quad(90\%\,\mathrm{CL}), \tag{19}$$

$$P(e\to e)/P(\mu\to\mu)=0.92\pm0.21, \tag{20}$$

for $L/E \sim 0.04$ m/MeV. The latter result follows from the excellent agreement between observed $e^{\pm}$ events and the calculated ν_e, $\bar{\nu}_e$ fluxes in the primary beams. At Fermilab the BNL-Columbia group finds[21] a weaker limit on $\nu_\mu \to \nu_e$ plus

$$P(\mu\to\tau)/P(\mu\to\mu)<0.025\quad(90\%\,\mathrm{CL}), \tag{21a}$$

while the Fermilab-Serpukhov-Moscow-Michigan group determines

$$P(\mu\to\tau)/P(\mu\to\mu)<0.0075\quad(90\%\,\mathrm{CL}) \tag{21b}$$

by exploiting y dependence.[22] Both of these limits are for $L/E \sim 0.04$ m/MeV also. Combining the bounds of Eqs. (18), (19), and (21b) leads to

$$P(\mu\to\mu)>0.99\quad(90\%\,\mathrm{CL}) \tag{22}$$

for $L/E \simeq 0.04$ m/MeV, assuming three neutrinos only.

D. Beam-dump measurements

In the CERN beam-dump experiments[23,24] prompt neutrinos are observed at distances $L \simeq 800$–900 m from the source; these neutrinos are presumed to come from charm-particle decays that are symmetrical between electron and muon modes. However, there is an apparent disparity between the number of prompt electron and muon events observed in the bubble-chamber experiment (after correcting for muon energy acceptance based on $\nu_\mu \to \mu^-$ and $\bar{\nu}_\mu \to \mu^+$ production and subtracting a calculated nonprompt background). The preliminary experimental result is[23]

$$R(e/\mu)\equiv N(e^{\pm})/N(\mu^{\pm})=0.59^{+0.35}_{-0.21}\quad(\mathrm{BEBC}). \tag{23}$$

This could be interpreted as a neutrino oscillation effect for $L/E \simeq 0.01$ m/MeV. Since we know that ν_μ oscillations are negligible in this range, these results suggest that $P(e\to e)$ is strongly suppressed. In the three-neutrino picture this implies strong $\nu_e \to \nu_\tau$ oscillations so that a fraction of the produced ν_e, $\bar{\nu}_e$ leads to $\tau^{\mp}$ events.

In the beam-dump experiments the antineutrino/neutrino flux ratio is not precisely known. However, oscillation calculations of observables averaged over ν and $\bar{\nu}$ fluxes turn out to be quite insensitive to relative contribution of the $\bar{\nu}$ components. For simplicity, therefore, we present our discussion in terms of neutrino components only, assuming identical ν_e and ν_μ flux and negligible ν_τ flux.

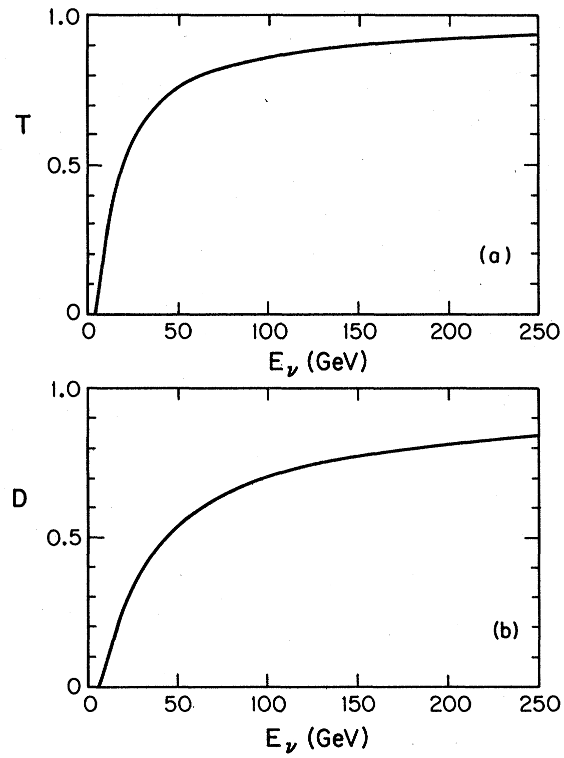

FIG. 2. (a) Ratio $T=\sigma^\tau/\sigma^e$ of inclusive τ to electron cross sections vs incident neutrino energy. (b) The average detection efficiency D of muons from τ production and decay divided by the fraction that would be detected in normal $\nu_\mu \to \mu^-$ production, assuming a muon acceptance cut $E_\mu > 5$ GeV.

For $\tau \to e$, μ branching fraction $B \simeq 0.17$, the ratio $R(e/\mu)$ is given by

$$R(e/\mu)=\frac{\langle P(e\to e)\sigma\rangle + B\langle P(e\to\tau)\sigma T\rangle}{\langle\sigma\rangle + B\langle P(e\to\tau)\sigma D\rangle}, \tag{24}$$

where σ is the inclusive charged-current cross section for e or μ and $T\equiv\sigma^\tau/\sigma^e$ is the relative suppression of τ production. The factor D is the fraction of muons detected from τ decays divided by the fraction that would be detected in normal $\nu_\mu \to \mu^-$ production. Figure 2 shows T and D versus neutrino energy, assuming a muon acceptance cut $E_\mu > 5$ GeV in D. In Eq. (24) $\langle\ \rangle$ denotes an average over the prompt neutrino spectrum. Taking mean values $\bar{T}$ and $\bar{D}$, we can invert Eq. (24) to obtain

$$\bar{P}(e\to e)=\frac{\langle P(e\to e)\sigma\rangle}{\langle\sigma\rangle}=\frac{R-B(\bar{T}-R\bar{D})}{1-B(\bar{T}-R\bar{D})}. \tag{25}$$

From the prompt-neutrino spectrum of Ref. 25 we calculate $\bar{T}\simeq 0.80$ and $\bar{D}\simeq 0.64$. The corresponding correlation between R and $\bar{P}(e\to e)$ is shown in Fig. 3(a). The experimental result in Eq. (23) suggests

$$\bar{P}(e\to e)=0.56^{+0.38}_{-0.24} \tag{26}$$

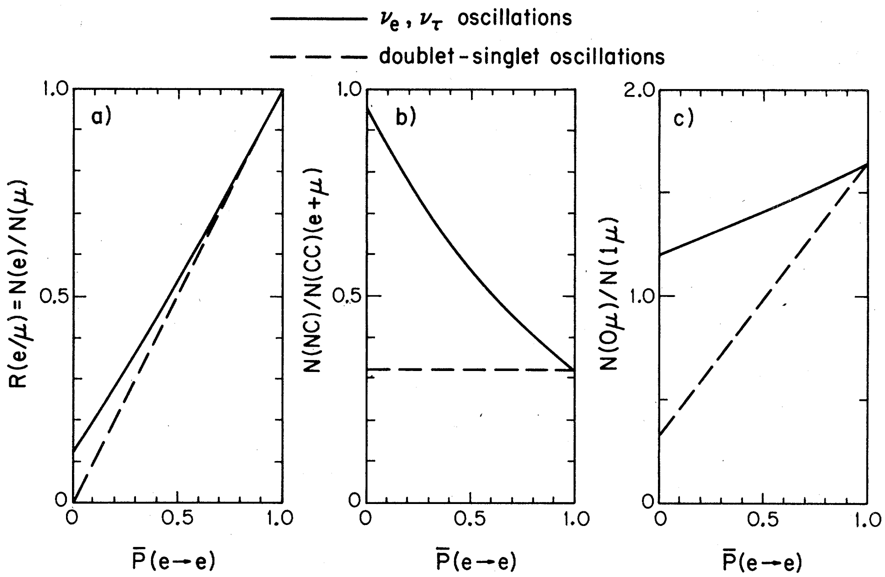

FIG. 3. Oscillation predictions for the CERN beam-dump observables (a) $R(e/\mu)=N(e)/N(\mu)$, (b) $N(\mathrm{NC})/N(\mathrm{CC})$ $(e+\mu)$, (c) $N(0\mu)/N(1\mu)$ vs the average probability $P(\bar{e}\to\bar{e})$. The solid curves denote flavor-changing $\nu_e \leftrightarrow \nu_e$ and $\nu_e \leftrightarrow \nu_\tau$ oscillation results. The dashed curves represent singlet-doublet mixing predictions.

for a prompt spectrum average in the range $L/E \sim 0.005-0.04$ m/MeV. We notice that Eq. (26) is barely compatible with Eqs. (20) and (22).

The bubble-chamber experiment also measures the ratio of neutral-current (NC) to charged-current (CC) $(e^\pm, \mu^\pm)$ events from prompt neutrinos. For $\nu_e \to \nu_e, \nu_\tau$ oscillations, the predicted ratio in terms of average values $\bar{P}(e\to e)$, $\bar{T}$, $\bar{D}$ is

$$\frac{N(\mathrm{NC})}{N(\mathrm{CC})}=\frac{2R(\mathrm{NC/CC})+(1-\bar{P})[\bar{T}-B(\bar{T}+\bar{D})]}{1+\bar{P}+B(1-\bar{P})(\bar{T}+\bar{D})}, \tag{27}$$

where $R(\mathrm{NC/CC})=\langle\sigma_{\mathrm{NC}}\rangle/\langle\sigma\rangle\simeq 0.32$. Figure 3(b) shows $N(\mathrm{NC})/N(\mathrm{CC})$ versus $\bar{P}(e\to e)$. For $\bar{P}(e\to e)$ given by Eq. (26), Eq. (27) would predict

$$\frac{N(\mathrm{NC})}{N(\mathrm{CC})}=0.53^{-0.18}_{+0.16} \tag{28}$$

for prompt neutrinos.

The beam-dump counter experiments measure the ratio $N(0\mu)/N(1\mu)$ of muonless to single-muon events. With e, τ neutrino oscillations the prediction is

$$\frac{N(0\mu)}{N(1\mu)}=\frac{2R(\mathrm{NC/CC})+\bar{P}+(1-\bar{P})(\bar{T}-B\bar{D})}{1+B(1-\bar{P})\bar{D}}. \tag{29}$$

Figure 3(c) shows this ratio versus $\bar{P}$.

An alternative possibility for explaining beam-dump results are oscillations which mix doublet and singlet electron neutrinos, and thus deplete the ν_e beam, as discussed in Ref. 8. The predictions based on doublet-singlet oscillations in the electron family are

$$\begin{aligned} &R(e/\mu)=\bar{P}, \\ &\frac{N(\mathrm{NC})}{N(\mathrm{CC})}\simeq 0.32, \\ &R\left(\frac{0\mu}{1\mu}\right)\simeq 0.32(1+\bar{P})+\bar{P}. \end{aligned} \tag{30}$$

These predictions are illustrated by the dashed curves in Fig. 3. In general, both doublet-singlet and flavor-changing oscillations could be present.

The preceding oscillation predictions for beam-dump results were expressed in terms of the average probability for ν_e depletion. Figure 4 shows $\bar{P}(e\to e)$ versus δm^2 for the leading oscillation, with mixing angles corresponding to $\sin^2 2\alpha=0.25$, 0.5, 0.75, and 1.0. Here $\bar{P}$ is averaged over the spectrum of Ref. 25. The experimental results in Eqs. (23) and (26) suggest a leading $\delta m^2 \gtrsim 50$ eV^2.

E. Meson-factory experiments

The decays of stopped pions and muons at meson factories provide characteristic monoenergetic ν_μ, $\bar{\nu}_\mu$ and continuum ν_μ, $\bar{\nu}_\mu$, ν_e, $\bar{\nu}_e$ fluxes in the 0–50 MeV range.

An experiment at LAMPF using ν_e and $\bar{\nu}_\mu$ fluxes from μ^+ decay has found[26]

$$P(e\to e)=1.1\pm 0.4, \tag{31}$$

$$P(\bar{\mu}\to\bar{e})<0.065\ \ (90\%\ \mathrm{CI}) \tag{32}$$

at $L/E\sim 0.3$ m/MeV.

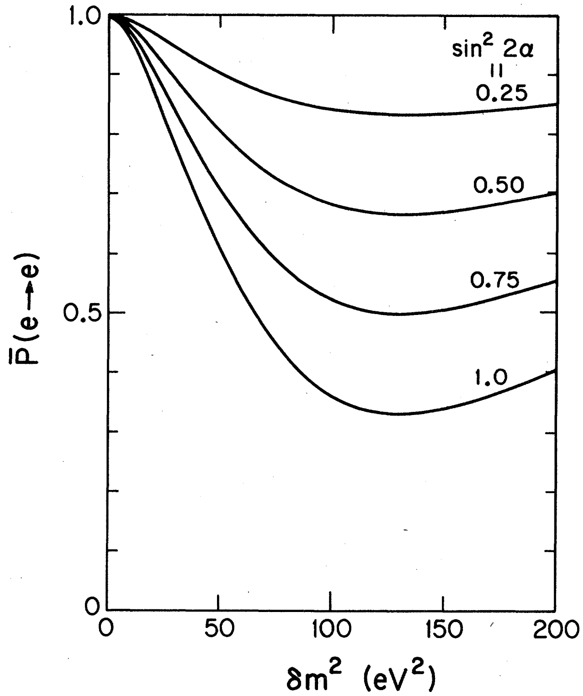

FIG. 4. Average probability $\bar{P}(e\rightarrow e)$ for the CERN beam-dump experiment vs δm^2, for various mixing parameters $\sin^2 2\alpha$.

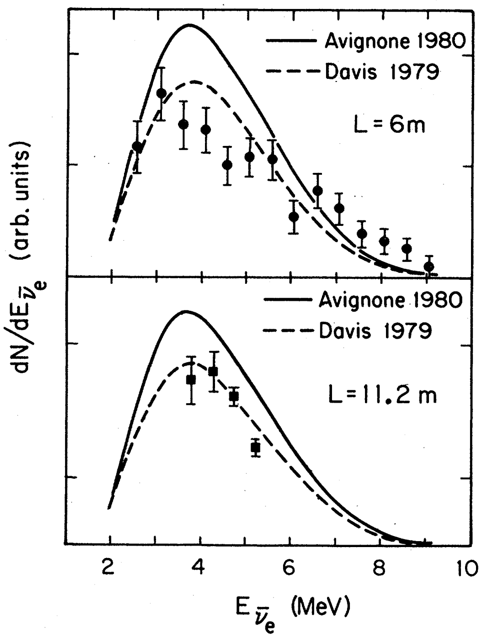

FIG. 5. Comparison of reactor flux measurements (Ref. 27) with theoretical fission spectra (Refs. 28 and 29).

F. Reactor experiments

Nuclear fission reactors provide copious fluxes of $\bar{\nu}_e$ in the few-MeV range; their transmission can be monitored in various ways.

1. Proton target

The inverse-β-decay process $\bar{\nu}_e + p \rightarrow e^+ + n$ is a convenient way to detect $\bar{\nu}_e$, above the threshold 1.8 MeV. Comparing the observed rate with the rate calculated from the fission spectrum gives a measurement of $P(\bar{e}\rightarrow\bar{e})$, subject to theoretical uncertainties in the fission spectrum.

Reines *et al.*[27] have measured $\bar{\nu}_e$ fluxes at $L=6$ and 11.2 m from the center of a cylindrical reactor core (5 m diameter, 5 m high). Figure 5 shows a comparison of these data with two choices of theoretical fission spectra, due to Avignone and Greenwood[28] and to Davis *et al.*[29] These spectra do not account for the $L=6$ m measurements for $E > 6$ MeV, where $P(\bar{e}\rightarrow\bar{e})$ apparently exceeds 1; the disagreement is worse for the spectrum of Davis *et al.* The determinations[3] of $P(\bar{e}\rightarrow\bar{e})$ based on these theoretical spectra are shown in Fig. 6. Here the horizontal error bars represent the rms spread due to reactor core size. This figure suggests a strong oscillation with one node near $L/E = 1.3$ m/MeV; to fit this as a leading-oscilla-

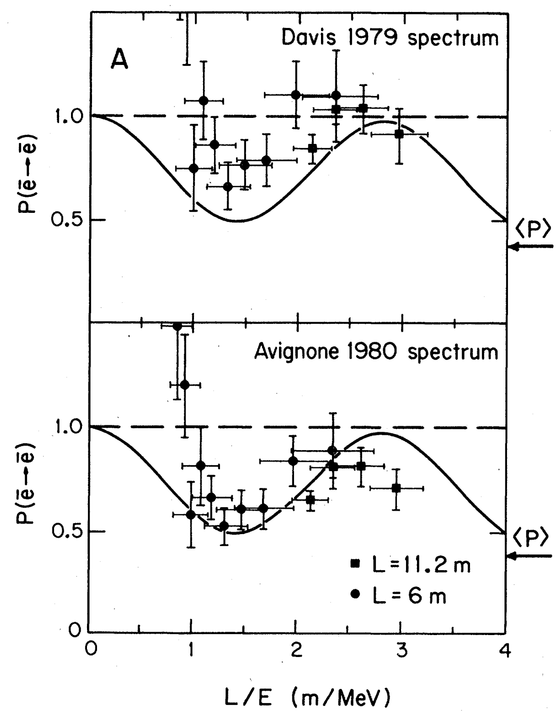

FIG. 6. Transition probability $P(\bar{e}\rightarrow\bar{e})$ versus L/E deduced from the ratio of observed to expected $\bar{\nu}_e$ reactor flux of Fig. 5. The curve represents solution A of Eq. (38).

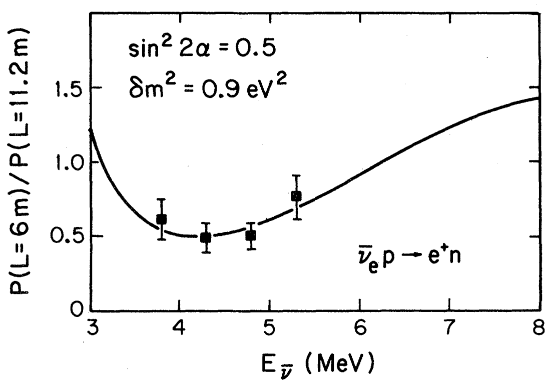

FIG. 7. Ratio of $P(\bar{e}\to\bar{e})$ at $L = 6$ and 11.2 m versus antineutrino energy $E_{\bar{\nu}}$. The overall normalization of the data ratios is chosen to best match the theory ratios.

tion effect [see Eq. (15)] would require a leading eigenmass squared difference $\delta m^2 \sim 1\ \mathrm{eV}^2$ and substantial mixing, $\sin^2 2\alpha \sim 0.5$.

More conservatively, one might regard these data as indicating some general suppression of $P(\bar{e}\to\bar{e})$ without establishing the details. If so, two other types of interpretation are possible: the smooth onset of a longer-wavelength oscillation (with $\delta m^2 \sim 0.2\ \mathrm{eV}^2$) or the average effect of a shorter-wavelength oscillation (with $\delta m^2 \gg 1\ \mathrm{eV}^2$).

Spectrum uncertainties can be avoided in principle by studying $\bar{\nu}_e$ fluxes versus L at fixed E, rather than versus E at fixed L, i.e., by looking for deviations from the inverse square law.[30] The L dependences in different E bins will provide independent (and overlapping) determinations of $P(\bar{e}\to\bar{e})$ versus L/E—and also of the initial $\bar{\nu}_e$ spectrum shape at the source. So far no such systematic measurements have been presented. Meanwhile, however, we can study the ratio of counting rates in the 6- and 11.2-m experiments[27] (assuming optimistically that reactor conditions and counting efficiencies were comparable in these different circumstances); in the absence of oscillations this ratio should be a constant. Figure 7 shows some indication for deviation of this ratio from a constant, but with considerable uncertainties.

2. *Deuteron target*

Deuteron breakup by antineutrinos has both neutral-current (NC) and charged-current (CC) channels:

$$\bar{\nu} + d \to \bar{\nu} + p + n\,,$$
$$\bar{\nu}_e + d \to e^+ + n + n\,. \tag{33}$$

For flavor oscillations the NC reaction is the same for all flavors of the neutrino; hence it is immune to oscillations and can be used to monitor the initial $\bar{\nu}_e$ flux. The ratio of CC/NC rates, integrated over the $\bar{\nu}$ spectrum above their respective thresholds, therefore provides a means to extract $P(\bar{e}\to\bar{e})$ that is relatively insensitive to theoretical uncertainties in the spectrum shape. This approach has been followed in Refs. 19 and 31.

The integrated cross sections for deuteron disintegration have the form

$$\bar{\sigma} = \int_0^\infty dE_r \int_{E_{\mathrm{th}}}^\infty dE_{\bar{\nu}}\, \rho(E_{\bar{\nu}}) f(E_{\bar{\nu}}) \frac{d\sigma}{dE_r}\,, \tag{34}$$

where $\rho(E_{\bar{\nu}})$ is the $\bar{\nu}_e$ flux at $L = 0$ and $f = P(\bar{e}\to\bar{e})$ at $L/E_{\bar{\nu}}$ for the CC case and $f = \frac{1}{2}$ for the NC case. The variable E_r is the energy of relative motion of the final-state nucleons; the recoil energy of the two-nucleon system can be neglected to a 1% approximation. The differential cross sections are[32]

$$\frac{d\sigma}{dE_r} = \frac{2 g_A{}^2 G_F{}^2 m_N}{\pi^3} J_d{}^2(E_r)(E_{\bar{\nu}} - E_{\mathrm{th}}) \times [(E_{\bar{\nu}} - E_{\mathrm{th}})^2 - m^2]^{1/2} E_r{}^{1/2}\,, \tag{35}$$

where m_N is the nucleon mass and $m = m_e$ for the CC and $m = 0$ for the NC cases. The threshold energies are

$$E_{\mathrm{th}}^{\mathrm{CC}} = 4.030\ \mathrm{MeV} + E_r\,, \quad E_{\mathrm{th}}^{\mathrm{NC}} = 2.225\ \mathrm{MeV} + E_r\,, \tag{36}$$

with E_r in MeV units. In Eq. (35) the quantity J_d is the overlap integral of deuteron wave functions describing the ^3S ground state and the ^1S continuum state.[32] With the exponential falloff of $\rho(E_{\bar{\nu}})$ folded in, the dominant contribution to σ comes from $E_r \simeq 0.05$–0.1 MeV and $E_{\bar{\nu}} - E_{\mathrm{th}} \simeq 0.5$–$3.5$ MeV.[31] Thus oscillation effects can be measured in the range 4.6–7.6 MeV. The experiment of Reines *et al.* at $L \simeq 11.2$ m is sensitive to $P(\bar{e}\to\bar{e})$ over the range $L/E \simeq 1.5$–2.4 m/MeV which is the region where the $\bar{\nu}_e p \to e^+ n$ data in Fig. 6 show an oscillation effect.

The reported results are[19]

$$\bar{P}(\bar{e}\to\bar{e}) = \frac{[\bar{\sigma}(\mathrm{CC})/\bar{\sigma}(\mathrm{NC})]\ \mathrm{experiment}}{[\bar{\sigma}(\mathrm{CC})/\bar{\sigma}(\mathrm{NC})]\ \mathrm{theory}\ L=0} = \begin{cases} 0.38 \pm 0.21 & (\text{spectrum Ref. 28}) \\ 0.40 \pm 0.22 & (\text{spectrum Ref. 29})\,. \end{cases} \tag{37}$$

V. SOLUTIONS

To accommodate the solar-neutrino data we concentrate on solutions near the minimizing solution of Sec. III. We specify the mass ordering as $m_1 < m_2 < m_3$. For simplicity we assume $\delta m^2{}_{21} \ll \delta m^2{}_{31}$ and CP conservation ($\delta = 0$ or π). We choose θ_1, θ_3

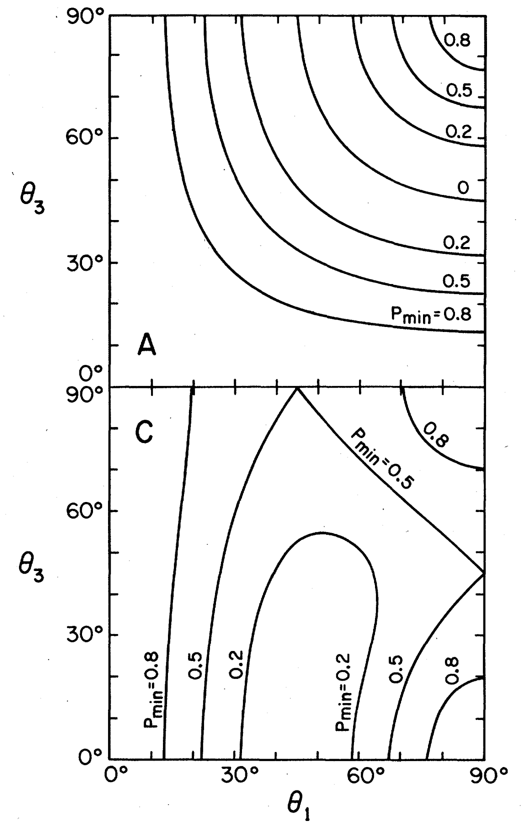

FIG. 8. Contour plot of the minimum value of $P(\bar{e}\to\bar{e})$ in the reactor range ($L/E \simeq 1$–3 m/MeV) versus the angles θ_1 and θ_3, for solutions A and C. The results for solution C are averaged over the leading oscillation.

to make $P(e\to e)$ close to its minimum and to fit the minimum value of $P(\bar{e}\to\bar{e})$ in the reactor range: see Fig. 8. Freedom remains in the choice of mass differences δm^2_{ij} and in the choice of θ_2 (this angle can be tuned to decouple ν_μ from the leading oscillation if necessary). Other data on neutrino oscillations then lead us to three major classes of solutions.

Class A. Here the leading oscillation is chosen to match the shape of $P(\bar{e}\to\bar{e})$ from reactor experiments with proton targets in Fig. 6; this fixes $\delta m^2_{31} \approx \delta m^2_{32} \simeq 0.9$ eV$^2 \gg \delta m^2_{21}$ and gives $\sin^2 2\alpha \sim 0.5$ for the leading-oscillation formulas of Eq. (15). With these parameters the various accelerator bounds on ν_μ oscillations are satisfied irrespective of the choice of β (or θ_2): see Fig. 9. However, given these mass scales there can be no large effects in the CERN beam-dump experiments, so the results in Eq. (26) must be ignored. All other data can be accommodated.

A typical solution of this type has parameters

$$\theta_1 = 50°,\quad \theta_2 = 20°,\quad \theta_3 = 30°,\quad \delta = 0,\quad \delta m^2_{31} = 0.9\ \text{eV}^2,\quad \delta m^2_{21} = 0.05\ \text{eV}^2. \tag{38}$$

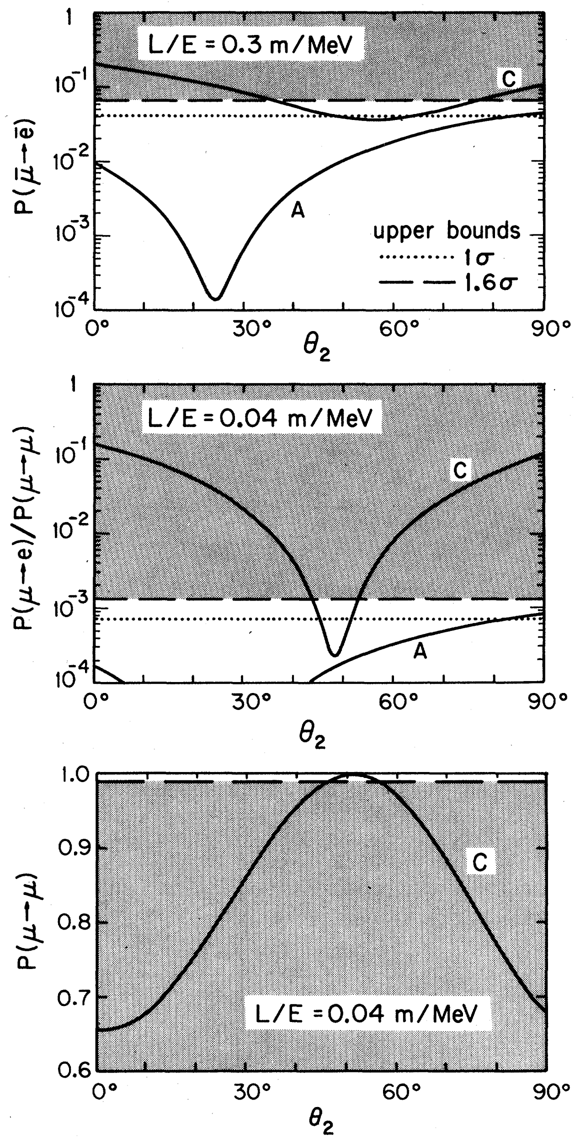

FIG. 9. Experimental bounds on $\nu_\mu\to\nu_e$ and $\nu_\mu\to\nu_\mu$ transitions compared with solutions A and C, allowing the angle θ_2 to vary. The shaded region is excluded at the 90% confidence level. For $P(\mu\to\mu)$ the prediction of solution A is essentially unity.

In this example θ_2 has been chosen to decouple ν_μ from the leading oscillation, which helps in satisfying the various bounds, but is not strictly necessary. The comparison with reactor proton-target data is shown in Fig. 6 and predictions for propagation probabilities $P(\alpha\to\beta)$ are shown versus L/E in Fig. 10. For reactor d disintegration this solution gives an average probability at L = 11.2 m of

$$\bar{P}(\bar{e}\to\bar{e}) = \begin{cases} 0.64 & \text{(spectrum Ref. 28)} \\ 0.68 & \text{(spectrum Ref. 29)}. \end{cases} \tag{39}$$

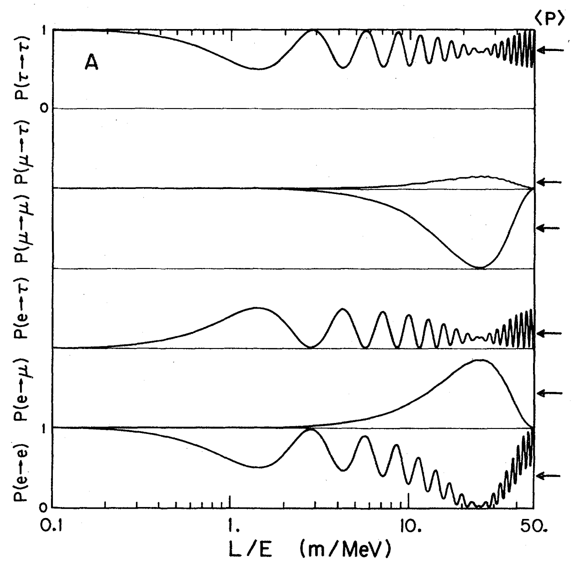

FIG. 10. Subasymptotic neutrino oscillations for all channels based on solution A in Eq. (38). Arrows on the right-hand side denote asymptotic mean values.

We note that for $\delta m^2 \simeq 0.7\ \mathrm{eV}^2$, the predicted $\bar{P}(\bar{e}\to\bar{e})$ values are 15 and 25% lower, respectively. For the solar-neutrino average solution A gives

$$\langle P(e\to e)\rangle = 0.39\,. \tag{40}$$

For deep-mine upward events (with $L/E \sim 10^3$ m/MeV) the vacuum oscillations in this solution have asymptotic averages

$$\begin{aligned} &\langle P(\nu_\mu\to\nu_\mu)\rangle = 0.50\,,\\ &\langle P(\nu_\mu\to\nu_e)\rangle = 0.43\,,\\ &\langle P(\nu_\mu\to\nu_\tau)\rangle = 0.07\,,\\ &\langle P(\nu_e\to\nu_\tau)\rangle = 0.19\,. \end{aligned} \tag{41}$$

Deep-mine horizontal events refer to the region $L/E \sim 10$ m/MeV, where the results depend rather critically on our choice of $\delta m^2{}_{21}$ and θ_2, which are essentially free in class A solutions.

Class B. Here the leading oscillation is supposed to be just beginning in the reactor range $L/E = 1.5-2.5$ m/MeV, giving some suppression of $P(\bar{e}\to\bar{e})$ but no detailed fit to present reactor data. This somewhat looser requirement implies a leading $\delta m^2 \sim 0.1-0.3\ \mathrm{eV}^2$ with $\sin^2 2\alpha \sim 0.5-1.0$. As with class A, these solutions easily satisfy accelerator bounds on ν_μ oscillations and predict negligible CERN beam-dump effects.

A typical solution of this class has parameters

$$\begin{aligned} &\theta_1 = 55°,\quad \theta_2 = 0,\quad \theta_3 = 45°,\quad \delta = 0\,,\\ &\delta m^2{}_{31} = 0.25\ \mathrm{eV}^2,\quad \delta m^2{}_{21} = 0.05\ \mathrm{eV}^2\,. \end{aligned} \tag{42}$$

The comparison with reactor proton-target data is

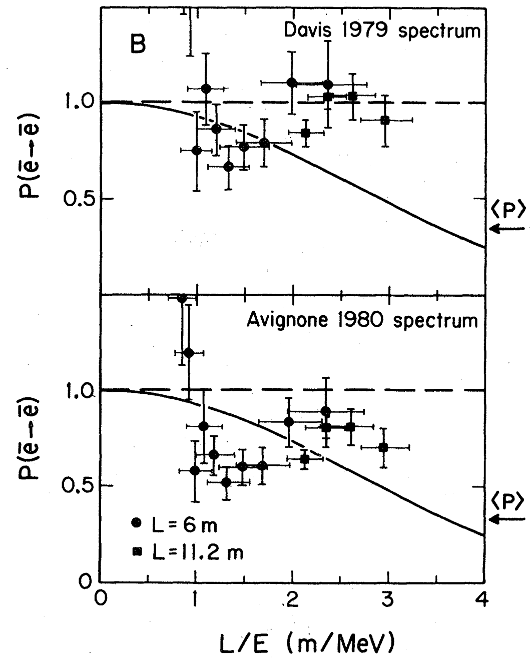

FIG. 11. Comparison of solution B in Eq. (42) with reactor proton-target data on $P(\bar{e}\to\bar{e})$.

shown in Fig. 11, and propagation probabilities are given in Fig. 12. For the reactor d-disintegration average this solution gives

$$\bar{P}(\bar{\nu}_e\to\bar{\nu}_e) = \begin{cases} 0.73 & (\text{spectrum Ref. 28}) \\ 0.70 & (\text{spectrum Ref. 29})\,, \end{cases} \tag{43}$$

while for the solar-neutrino and deep-mine upward

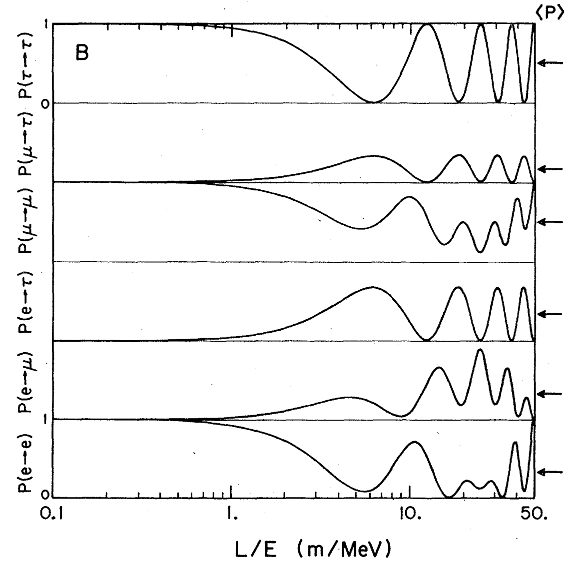

FIG. 12. Subasymptotic oscillations for solution B in Eq. (42).

event averages it gives

$$\langle P(\nu_e \to \nu_e)\rangle = 0.33\,,$$
$$\langle P(\nu_\mu \to \nu_\mu)\rangle = 0.50\,,$$
$$\langle P(\nu_\mu \to \nu_e)\rangle = 0.33\,, \qquad (44)$$
$$\langle P(\nu_\mu \to \nu_\tau)\rangle = 0.17\,,$$
$$\langle P(\nu_e \to \nu_\tau)\rangle = 0.33\,.$$

Class C. Here the leading oscillation is supposed to have $\delta m^2_{31} \simeq \delta m^2_{32} \gg 1$ eV^2, so that the reactor experiments are simply measuring the average effects of many short wavelength oscillations of which the details are not resolved. With bigger mass scales now permitted, a sizable effect in the CERN beam-dump experiments is no longer excluded; however, it is critical to tune θ_2 such that ν_μ decouples from the leading oscillations, in order to satisfy the accelerator bounds: see Fig. 9. (Such a solution with $U_{\mu 3} \simeq 0$ has been proposed by De Rûjula *et al.*,[4] in the beam-dump context.)

A typical solution of this kind is

$$\theta_1 = 30°,\quad \theta_2 = 50°,\quad \theta_3 = 55°,\quad \delta = 0\,,$$
$$\delta m^2_{31} = 50\ \text{eV}^2,\quad \delta m^2_{21} = 0.9\ \text{eV}^2\,. \qquad (45)$$

The comparison with reactor proton-target data is shown in Fig. 13 and propagation probabilities are shown in Fig. 14. For the reactor d-disintegration average this solution gives

$$\overline{P}(\bar\nu_e \to \bar\nu_e) = \begin{cases} 0.55 & \text{(spectrum Ref. 28)} \\ 0.56 & \text{(spectrum Ref. 29)}\,, \end{cases} \qquad (46)$$

while for the solar-neutrino and deep-mine upward event averages it gives

$$\langle P(\nu_e \to \nu_e)\rangle = 0.60\,,$$
$$\langle P(\nu_\mu \to \nu_\mu)\rangle = 0.81\,,$$
$$\langle P(\nu_\mu \to \nu_e)\rangle = 0.15\,, \qquad (47)$$
$$\langle P(\nu_\mu \to \nu_\tau)\rangle = 0.04\,,$$
$$\langle P(\nu_e \to \nu_\tau)\rangle = 0.25\,.$$

A brief summary and comparison follows.

(i) There may be some conflict between the reactor (proton-target) and beam-dump results. However, this conflict can be narrowly resolved by solution C.

(ii) Class A solutions take seriously the details of reactor data—especially the suggestion of a well-resolved oscillation—but if this is the leading mass scale, there should be no beam-dump effects.

(iii) Class B solutions take reactor (proton-target) data less seriously, as a longer wavelength effect, but thereby also fail to fit beam-dump results. They seem disfavored.

(iv) Class C represents a possible compromise,

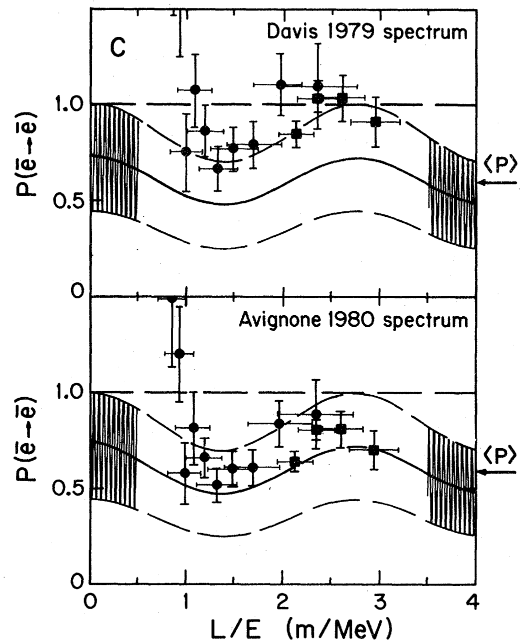

FIG. 13. Comparison of solution C in Eq. (45) with reactor proton-target data on $P(\bar e \to \bar e)$. The heavy solid curve denotes the average value of $P(\bar e \to \bar e)$ and the dashed curves represent the envelopes of the oscillations; parts of the short-wavelength oscillations are illustrated.

where reactor data are regarded as averages of short-wavelength unresolved oscillations. These solutions can fit beam-dump data.

(v) In the accelerator and meson-factory ranges of L/E, class C predicts many interesting effects which will serve as definitive tests. Class A predicts minimal effects and class B essentially no

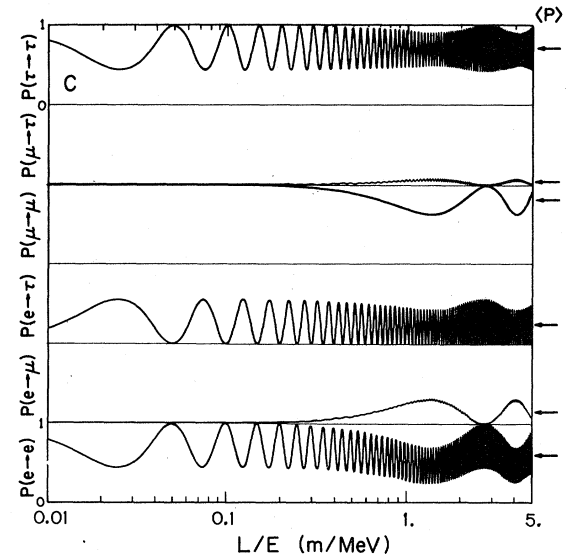

FIG. 14. Subasymptotic oscillations for solution C in Eq. (45).

effects at all here.

(vi) Deep-mine data will be very helpful in restricting parameters, including the nonleading mass difference $\delta m^2{}_{21}$.

ACKNOWLEDGMENTS

We acknowledge the participation of D. Cline in previous collaborations on this topic, which overlap with the considerations of this paper. We thank P. Langacker, J. Leveille, S. Pakvasa, and H. Wachsmuth for useful discussions. This research was supported in part by the University of Wisconsin Research Committee with funds granted by the Wisconsin Alumni Research Foundation, and in part by the Department of Energy under Contract No. DE-AC02 76ER00881, COO-881-151.

---

[1]Neutrino oscillations were first considered by Z. Maki, M. Nakagawa, and S. Sakata, Prog. Theor. Phys. 28, 870 (1962) and B. Pontecorvo, Zh. Eksp. Teor. Fiz. 53, 1717 (1967) [Sov. Phys. JETP 26, 984 (1968)].

[2]For a recent review and references see S. M. Bilenky and B. Pontecorvo, Phys. Rep. 41C, 225 (1978).

[3]V. Barger, D. Cline, R. J. N. Phillips, and K. Whisnant, Phys. Lett. 93B, 194 (1980).

[4]A. De Rújula, M. Lusignoli, L. Maiani, S. T. Petcov, and R. Petronzio, Nucl. Phys. B168, 54 (1980).

[5]A. K. Mann and H. Primakoff, Phys. Rev. D 15, 655 (1977).

[6]J. N. Bahcall and H. Primakoff, Phys. Rev. D 18, 3463 (1978); A. Zee, Univ. of Pennsylvania Report No. UPR-0150T, 1980 (unpublished).

[7]S. M. Bilenky and B. Pontecorvo, Lett. Nuovo Cimento 17, 569 (1976).

[8]V. Barger, P. Langacker, J. P. Leveille, and S. Pakvasa, Phys. Rev. Lett. 45, 692 (1980).

[9]L. Wolfenstein, Phys. Rev. D 17, 2369 (1978).

[10]M. Kobayashi and T. Maskawa, Prog. Theor. Phys. 49, 652 (1973).

[11]R. Davis, Jr., in *Proceedings of the Brookhaven Solar Neutrino Conference* (BNL, Upton, New York, 1978), Vol. 1, p. 1.

[12]J. Bahcall, Space Sci. Rev. 24, 227 (1979); V. Gribov and B. Pontecorvo, Phys. Lett. 28B, 493 (1969); J. Bahcall and S. C. Frautschi, *ibid.* 29B, 623 (1969).

[13]S. Nussinov, Phys. Lett. 63B, 201 (1976).

[14]N. Cabibbo, Phys. Lett. 72B, 333 (1978).

[15]L. Wolfenstein, Phys. Rev. D 18, 958 (1978).

[16]R. Ehrlich, Phys. Rev. D 18, 2323 (1978); R. Barbieri *et al.*, Phys. Lett. 90B, 249 (1980).

[17]M. R. Krishaswamy *et al.*, Proc. R. Soc. London A323, 489 (1971).

[18]M. F. Crouch *et al.*, Phys. Rev. D 18, 2239 (1978); F. Reines, *Sixteenth International Cosmic Ray Conference, Kyoto, 1979, Conference Papers* (Institute of Cosmic Research, Univ. of Tokyo, 1979); see also remarks in Ref. 19.

[19]F. Reines, H. W. Sobel, and E. Pasierb, Univ. California-Irvine Report, 1980 (unpublished); H. W. Sobel, talk at the XXth International Conference on High Energy Physics, Madison, Wisconsin, 1980 (unpublished).

[20]J. Blietschau *et al.*, Nucl. Phys. B133, 205 (1978).

[21]A. M. Cnops *et al.*, Phys. Rev. Lett. 40, 144 (1978).

[22]B. P. Roe (private communication).

[23]H. Wachsmuth, in *Proceedings of Workshop on Production of New Particles in Super High Energy Collisions*, edited by V. Barger and F. Halzen (University of Wisconsin, Madison, 1980), and private communication; P. O. Hulth, talk at the XXth International Conference on High Energy Physics, Madison, Wisconsin, 1980 (unpublished).

[24]H. Wachsmuth *et al.*, British European Bubble Chamber (BEBC) collaboration (unpublished); K. Winter, CERN-Hamburg-Amsterdam-Rome-Moscow (CHARM) collaboration (unpublished); J. Steinberger *et al.*, CERN-Dortmund-Heidelberg-Saclay (CDHS) collaboration (unpublished).

[25]An estimate of the prompt-neutrino spectrum by G. Conforto and F. Ferroni is given in Ref. 4.

[26]S. E. Willis *et al.*, Phys. Rev. Lett. 44, 522 (1980).

[27]F. Nezrick and F. Reines, Phys. Rev. 142, 852 (1966); F. Reines, in *Unification of Elementary Forces and Gauge Theories*, proceedings of the Ben Lee Memorial International Conference on Parity Nonconservation, Weak Neutral Currents, and Gauge Theories, Fermilab, 1977, edited by D. B. Cline and F. E. Mills (Harwood Academic, New York, 1979), p. 103.

[28]F. T. Avignone III and Z. D. Greenwood, Phys. Rev. C 22, 594 (1980).

[29]B. R. Davis, P. Vogel, F. M. Mann, and R. E. Schenter, Phys. Rev. C 19, 2259 (1979).

[30]V. Barger *et al.*, UW-Madison Report No. COO-881-148, 1980 (unpublished).

[31]V. Barger *et al.*, J. Phys. G (to be published).

[32]S. A. Fayans, L. A. Mikaelian, and Y. L. Dobryin, J. Phys. G 5, 209 (1979); T. Ahrens and L. Gallaher, Phys. Rev. D 20, 2714 (1979).

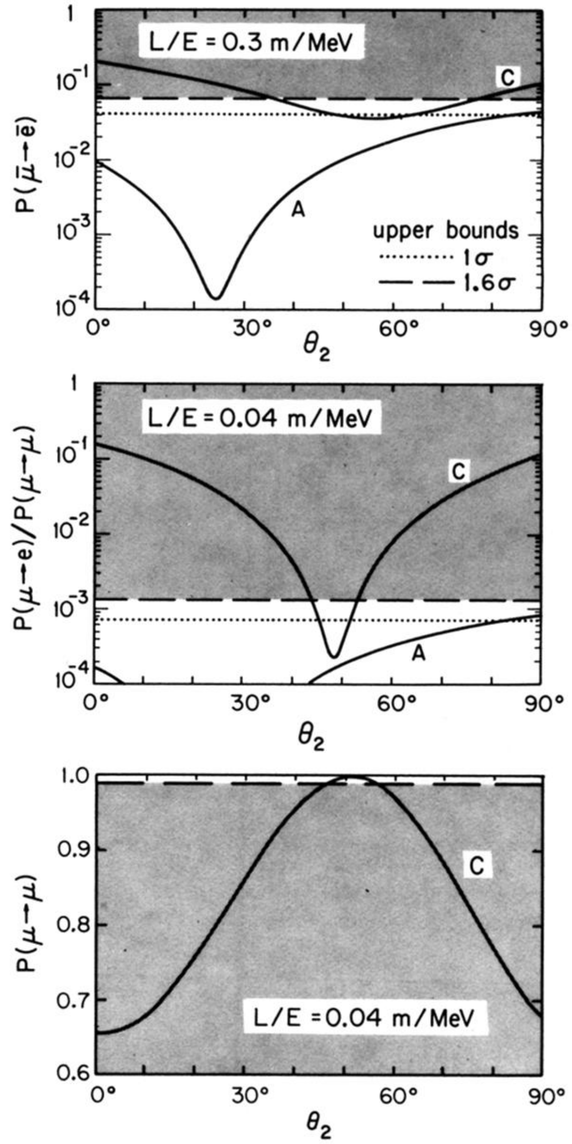

FIG. 9. Experimental bounds on $\nu_\mu \to \nu_e$ and $\nu_\mu \to \nu_\mu$ transitions compared with solutions A and C, allowing the angle θ_2 to vary. The shaded region is excluded at the 90% confidence level. For $P(\mu \to \mu)$ the prediction of solution A is essentially unity.